Acta Biochim Biophys Sin, 2017, 49(10), 926–934
doi: 10.1093/abbs/gmx094
Advance Access Publication Date: 1 September 2017
Original Article

Original Article

Knockdown of SLC39A7 inhibits cell growth and induces apoptosis in human colorectal cancer cells

Nengquan Sheng[1,†], Li Yan[1,†], Weiqiang You[1], Gewen Tan[1], Jianfeng Gong[1], Hongqi Chen[1], Yi Yang[2], Landian Hu[3,*], and Zhigang Wang[1,*]

[1]Department of General Surgery, Shanghai Jiao Tong University Affiliated Sixth People's Hospital, Shanghai 200233, China, [2]Department of Oncological Surgery, Kunshan Hospital of Traditional Chinese Medicine Affiliated to Nanjing University of Chinese Medicine, Kunshan 215300, China, and [3]The Key Stem Cell Laboratory, Institute of Health Sciences, Shanghai Jiao Tong University School of Medicine and Shanghai Institutes for Biological Sciences, Chinese Academy of Sciences, Shanghai 200031, China

[†]These authors contributed equally to this work.
*Correspondence address: Tel/Fax: +86-21-24058549; Email: surlab@hotmail.com (Z.W.)/Tel: +86-21-54923330; Email: ldhu2013@163.com (L.H.)

Received 2 July 2017; Editorial Decision 30 July 2017

Abstract

SLC39A7 (zip7) is a zinc transporter that plays a key role in intestinal epithelial self-renewal. However, little is known about SLC39A7 in colorectal cancer. To assess the biological function of SLC39A7 in colorectal cancer, the expression of SLC39A7 in human colorectal tumors and five colorectal cancer cell lines were evaluated by Oncomine Cancer Microarray Database and western blot analysis. In addition, short hairpin RNAs specifically targeting SLC39A7 were transfected into HCT116 and SW1116 cells to knockdown SLC39A7 expression. Then, the effects of SLC39A7 knockdown on colorectal cancer cells were detected by 3-(4,5-dimethylthiazol-2-yl)-2, 5-diphenyltetrazolium bromide, colony-forming assay and flow cytometry. Our results showed that colorectal tumors have higher expression levels of SLC39A7 than normal colon tissues. Knockdown of SLC39A7 exhibited a significant decrease in cell viability and proliferation of colorectal cancer cells. It was also shown that knockdown of SLC39A7 interfered with cell cycle progression and induced G2/M cell cycle arrest, as well as boosted early and late apoptosis in colorectal cancer cells. Furthermore, downregulation of SLC39A7 promoted the cleavage of PARP and enhanced the expression of Bad, Caspase-9, and cleaved-Caspase-3, as well as suppressed Bcl-2 expression. In conclusion, our results suggest that SLC39A7 plays a crucial role in the proliferation and survival of colorectal cancer cells, which associates with colorectal tumorigenesis.

Key words: SLC39A7, cell viability, proliferation, apoptosis

Introduction

Colorectal cancer is one of the most common lethal human cancers worldwide [1]. It has become the second-leading cause of cancer-related death in USA and has a 5-year survival rate of 65% [2]. Local recurrence, distant metastasis, and extremely rapid development of process are the key characteristics of colorectal cancer [3]. Surgical resection,

systemic chemotherapy, and radioembolism are major strategies for treating this disease; however, high mortality and poor prognosis are still unsolved serious clinical problems [2,3]. Therefore, elucidating the molecular mechanisms involved in the evolution of colorectal cancer is urgently needed, which may facilitate the development of novel therapeutic agents.

Zinc, an essential trace element for normal biological functions of cells, including differentiation, DNA synthesis, and mitosis [4]. It is a structural component of a wide range of cellular proteins, such as structural proteins, transcription factors, and enzymes that responsible for cell signal transduction pathways [5]. Previous studies have revealed that zinc is associated with proliferation, invasion, and apoptosis of many types of human cancer cells [5].

Intracellular zinc homeostasisis controlled by zinc importers (SLC39A/Zip) and exporters (SLC30Aa/ZnT) [6]. SLC39A7 (ZIP7) is a member of LIV-1 subfamily of zinc transporters, which contributes to the homeostatic maintenance of zinc through affecting storage and intracellular zinc redistribution [7]. It is localized mainly to the Golgi apparatus and/or endoplasmic reticulum [8]. SLC39A7 expression is remarkably upregulated in breast cancer cells and gastric tumor model [9]. Elevated level of SLC39A7 promotes growth and invasion through activation of growth factor receptor signaling such as epithelial growth factor receptor (EGFR), insulin-like growth factor receptor 1 (IGF-1R), and Src in tamoxifen-resistant MCF-7 cells [8]. Recent evidence in MCF-7 cells showed that the phosphorylation of SLC39A7 by CK2 leads to SLC39A7-mediated zinc release from the endoplasmic reticulum and induction of multiple downstream pathways that responsible for cell proliferation and migration [10]. In fact, SLC39A7 is also considered as a potential target of Wnt/β-catenin, which governs the maintenance of intestinal stem cells and is widely implicated in numerous malignancies [9]. However, the biological function of SLC39A7 in colorectal cancer has never been reported.

Considering the role of SLC39A7 in controlling zinc concentration, and its implication in tamoxifen-resistant MCF-7 cells invasion and proliferation, we supposed that SLC39A7 may also be associated with colorectal tumorigenesis. In this study, SLC39A7 expression pattern in colorectal cancer tissues and five cell lines were examined. Stable knockdown of SLC39A7 in HCT116 and SW1116 cells was achieved by using short hairpin RNAs (shRNAs). The effects of downregulation of SLC39A7 on cell viability, colony-forming ability, cell cycle distribution, and apoptosis were elucidated. This study will provide a better understanding of colorectal cancer tumorigenesis and development.

Materials and Methods

Oncomine analysis

The Oncomine Premium Database (http://www.oncomine.org) was accessed to compare the expression of SLC39A7 in colorectal cancer with that in normal tissues using two independent datasets, i.e. Kaiser's colon dataset [11] and Ki's colon dataset [12], according to the standard procedures as described by Rhodes *et al.* [13]. SLC39A7 expression values were presented in $\log_2$ median-centered intensity.

Cell culture

The colorectal cancer cells (RKO, DLD-1, SW116, HCT116, and LOVO) and human embryonic kidney cells 293 T (HEK293T) were obtained from the Cell Bank of Chinese Academy of Science (Shanghai, China). DLD-1, SW1116, and HEK293T cells were cultured in Dulbecco's modified Eagle's medium (Hyclone, Logan, USA) containing 10% fetal bovine serum (FBS; Biowest, Spain). The HCT1116 cells were maintained in PPMI 1640 medium (Hyclone) supplemented with 10% FBS. The RKO cells were grown in Hams F12 medium (JRH Biosciences, Lenexa, USA) with 10% FBS. Cultures were incubated at 37°C in a humidified atmosphere of 5% CO_2–95% air.

Lentivirus production and infection

The SLC39A7 targeting sequence 5′-GCCTTTCTTGTCGTGGAG AAA-3′ was constructed into the pGreenPuro™ shRNA Cloning and Expression Lentivector (SBI, Palo Alto, USA). Nonhunman targeting sequence, 5′-TTCTCCGAACGTGTCACGT-3′, was used as negative control. To generate the lentivirus, the plasmids pGp-shSLC39-A7 or pGp-shCon vector were transfected into HEK293T cells with second-generation packaging construct pCMV-dR8.74 (helper vectors for packaging; Hollylab, Shanghai, China) and pMD2G (vector encoding for envelop protein; Hollylab) according to the manufacturer's instruction.

The supernatant containing lentivirus was harvested and filtered through a 0.45-μm pore size HA Millipore filters (Millipore Corp., Bedford, USA) to remove cell debris. HCT116 and SW1116 cells were seeded in wells of 6-well plate at an inoculation density of 50,000 and 30,000 cells/well, respectively, then infected with the virus at a multiplicity of infection of 40 and 25, respectively. After amplification for 96 h, the GFP-positive cells and infection efficiency were observed under a microscope (Olympus, Tokyo, Japan).

Quantitative real-time PCR

Total RNA was extracted using RNeasy Mini kit (Qiangen, Valencia, USA) and cDNA was synthesized using PrimeScript RT Reagent Kit (TaKaRa, Dalian, China) according to the manufacturer's instructions. The primer sequences were used as follows: *SLC39A7* (NCBI accession number, NM_006,979) forward primer, 5′-CTGGAGCGGTGAGAAT GAGAGG-3′; *SLC39A7* reverse primer, 5′-ACTGGTGGGAGAAA GGAAACTGG-3′; *actin* forward primer, 5′-GTGGACATCCGCAAA GAC-3′; *actin* reverse primer, 5′-AAAGGGTGTAACGCAACTA-3′. For the quantification of SLC39A7 mRNA expression, quantitative real-time PCR (RT-qPCR) was performed using SYBR Green PCR Master Mix (TaKaRa) and actin as an internal control. Target sequences were amplified on a Bio-Rad CFX96 real-time System (Bio-Rad, Hercules, USA) at 95°C for 1 min, denaturation 95°C for 5 s, followed by 40 cycles of 60°C for 20 s. The fold change in the level of SLC39A 7 mRNA was analyzed using the $2^{-\Delta\Delta CT}$ method.

Western blot analysis

Cells were lysed with M-PER protein extraction reagents (Pierce, Rockford, USA) with protease inhibitor cocktail (Roche Diagnostics, Indianapolis, USA). The protein content in the cell lysate was determined by using BCA protein assay reagent kit (Pierce). Thirty micrograms of protein samples were separated on 10% SDS-PAGE and transferred to PVDF membranes. The membranes were blocked with 5% fat-free milk in TBS and incubated with primary antibodies against SLC39A7 (1:2000; Proteintech, Chicago, USA), Bad (1:500; Proteintech), Bcl-2 (1:500; Proteintech), Caspase-3 (1:1000; Proteintech), Caspase-9 (1:1000; Proteintech), PARP (1:1000; Cell Signaling Technology, Boston, USA) at 4°C overnight. Anti-GAPDH antibody (1:100,000; Proteintech) was used as an internal standard for the normalization of

protein expression levels. The membranes were probed with HRP-conjugated goat anti-rabbit or mouse antibody (1:5000 dilution; Santa Cruz Biotech, Santa Cruz, USA). The chemiluminiscence signal was detected using ECL western blotting detection kit (Amersham Biosciences, Buckinghamshire, UK).

3-(4,5-Dimethylthiazol-2-yl)-2, 5-diphenyl-tetrazolium bromide assay

HCT116 and SW1116 cells were seeded in 96-well plates and incubated for 5 days to establish exponential growth (initial cell density was 2200 cells/well for HCT116 and 2500 cells/well for SW1116). Then, 20 µl of 3-(4,5-dimethylthiazol-2-yl)-2, 5-diphenyl-tetrazolium bromide (MTT) was added into each well at different time points. After 2 h of incubation, the entire supernatant was discarded and 100 µl of acidified isopropyl alcohol (10% SDS, 5% isopropanol, and 0.01 mM HCl) was added into each well of the plate. Absorbance values at 595 nm were measured with a microplate reader.

Colony formation assay

For the colony formation assay, HCT116 and SW1116 cells were seeded at a density of 500 cells per well in 6-well plates and cultured in complete medium for 8 and 10 days, respectively. The medium was changed to fresh medium every three days. Cells were washed with PBS, fixed with 4% paraformaldehyde for 15 min and stained with 1% crystal violet for 30 min. Colonies were washed, then images were captured under the microscope and the number of colonies was counted.

Cell cycle assay

To detect cell cycle progression, HCT116 and SW1116 cells were grown in 6-cm dishes at a density of 200,000 per dish. After the incubation period, cells were harvested, fixed with 70% ethanol at 4°C, and treated with NaCl/PI staining solution (100 µg/ml RNase A and 50 µg/ml propidium iodide). After 1 h of incubation at 37°C, analysis was performed on a FACSCalibur flow cytometer (BD, Franklin Lakes, USA). The fractions of cells at the G0/G1, S and G2/M phases were analyzed and calculated with the Flowjo 7.6 software.

Apoptosis assay

Cells undergoing apoptosis was determined by Annexin V-APC/7AAD double staining using apoptosis detection kit (KeyGEN, Nanjing, China) and performed on a FACSCalibur flow cytometer according to the manufacturer's instructions. The apoptotic cells were divided into two groups: early apoptosis (Annexin V+/7AAD–) and late apoptosis (Annexin V+/7AAD+).

Statistical analysis

Experiments were repeated three times. The differences between groups were evaluated for statistical significance with t test and expressed as the mean ± standard deviation (SD). Data were analyzed using Excel software (Microsoft, Redmond, USA). $P < 0.05$ was considered as statistically significant.

Results

SLC39A7 is upregulated in human colorectal cancers

To explore the correlation between SLC39A7 and colorectal cancer, the expression of SLC39A7 in normal and colorectal cancer tissues were examined by analyzing an Oncomine gene array database (http://www.oncomine.org) using two independent datasets. Analysis of Kaiser's colon dataset (**Fig. 1A**) showed that SLC39A7 mRNA expression in colon adenocarcinoma ($n = 41$, $P = 0.009$), rectal mucinous adenocarcinoma ($n = 4$, $P = 0.014$) and colon mucinous adenocarcinoma ($n = 13$, $P = 0.001$) exhibited a significant increase when compared with those in normal tissues ($n = 5$). From Ki's colon dataset (**Fig. 1B**), SLC39A7 mRNA expression was

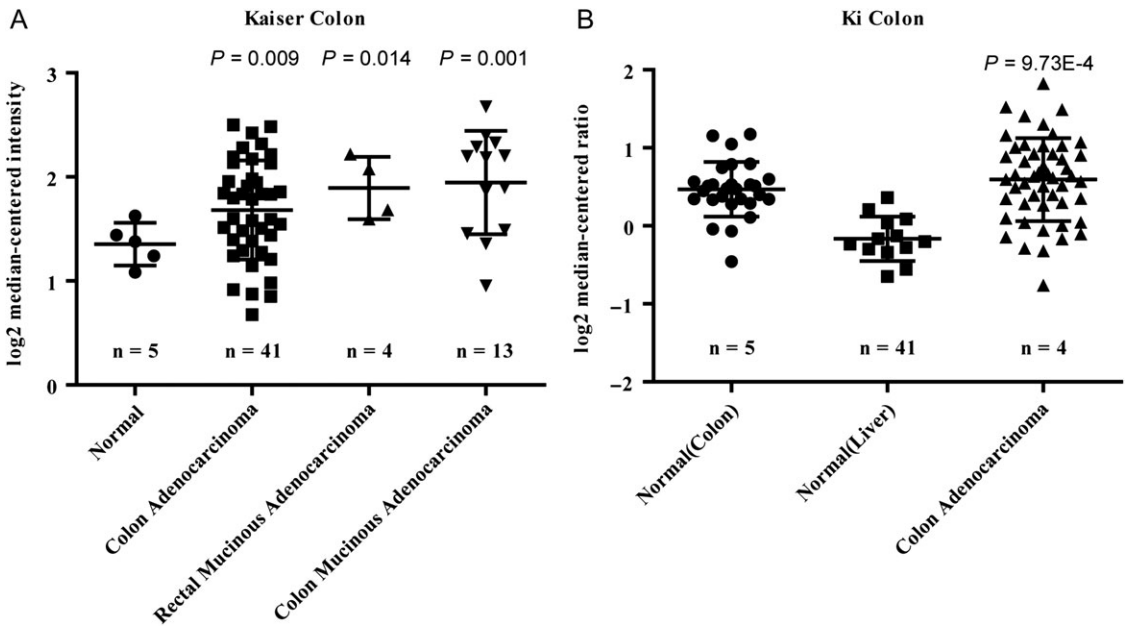

Figure 1. SLC39A7 is upregulated in colorectal cancer tissues The specific expression profiles of SLC39A7 mRNA were obtained from Kaiser's colon dataset (A) and Ki's colon dataset (B).

also found to be upregulated in colon adenocarcinoma ($n = 50$, $P = 0.000973$) when compared with those in normal tissues of colon ($n = 28$) and liver ($n = 13$). Therefore, the expression profiles from both datasets in Oncomine show that the SLC39A7 mRNA level is obviously higher in colorectal cancer tissues than in normal colon tissues.

Transfection of shSLC39A7 significantly suppressed SLC39A7 mRNA and protein expression

First, western blot analysis was carried out to examine the endogenous SLC39A7 protein expression level in five colorectal cancer cell lines. Our data revealed that the relative protein expression levels of SLA39A7 in RKO, DLD-1, SW1116, HCT116, and LOVO cells was 0.62, 0.66, 0.51, 0.72, and 0.59, respectively (**Supplementary Fig. S1A**). There was no significant difference among these five cells in the expression of SLC39A7 protein, therefore, only two representative colorectal cancer cell lines, i.e. SW1116 and HCT116, were selected for the subsequent experiments.

Next, distinct shRNAs specifically targeting SLC39A7 were designed and cloned to prepare the lentivirus. Then, HCT116 cells were infected with lentivirus carrying shSLC39A7. Four days after infection, successful and highly efficient infection were achieved with more than 80% GFP+ cells observed for both shRNAs and there was no significant difference in the transfection efficiency between these two shRNAs (**Supplementary Fig. S1B**), Therefore, SW1116 and HCT116 cells transfected with shSLC39A7 were systematically analyzed in the subsequent experiments.

To assess the knockdown efficiency of SLC39A7 in mRNA and protein levels, RT-qPCR and western blot analysis were performed. The results showed that a 73.5% decrease were observed at SLC39A7 mRNA level in HCT116 cells transfected with shSLC39A7 compared with HCT116 cells transfected with shCon (**Fig. 2A**). When SW1116 cells were transfected with shSLC39A7, the expression level of SLC39A7 mRNA was decreased by 53.3% compared with cells transfected with shCon (**Fig. 2B**). Consistently, the endogenous SLC39A7 protein level was significantly decreased by transfection with shSLC39A7 in both cell lines (**Fig. 2C,D**). These results demonstrated that both the SLC39A7 transcriptional level and translational level were obviously reduced by SLC39A7-specific lentivirus treatment.

SLA39A7 knockdown strongly inhibited the cell proliferation and colony formation

Four days after infection, the cell viability was measured for five consecutive days by MTT assay. On Day 4, the number of viable HCT116 cells infected with shSLC39A7 was reduced by 51.2% compared with cells transfected with shCon, and this trend was more obvious on Day 5 (**Fig. 3A**). On the fourth and fifth day, the viability of SW1116 cells was decreased by 28.0% and 31.6% in shSLC39A7-transfected groups compared with the shCon-transfected group (**Fig. 3A**). Additionally, colony-forming activity was carried out to identify the impact of SLC39A7 knockdown on the proliferation of colorectal cancer cells. As shown in **Fig. 3B–D**, knockdown of SLC39A7 by shRNA greatly inhibited colony size and decreased the number of colonies. Compared with the shCon group, shSLC39A7 transfection severely decreased the number of colonies by 96.6% in HCT116 cells (**Fig. 3C**). Similarly, a nearly 62.1% reduction was found in

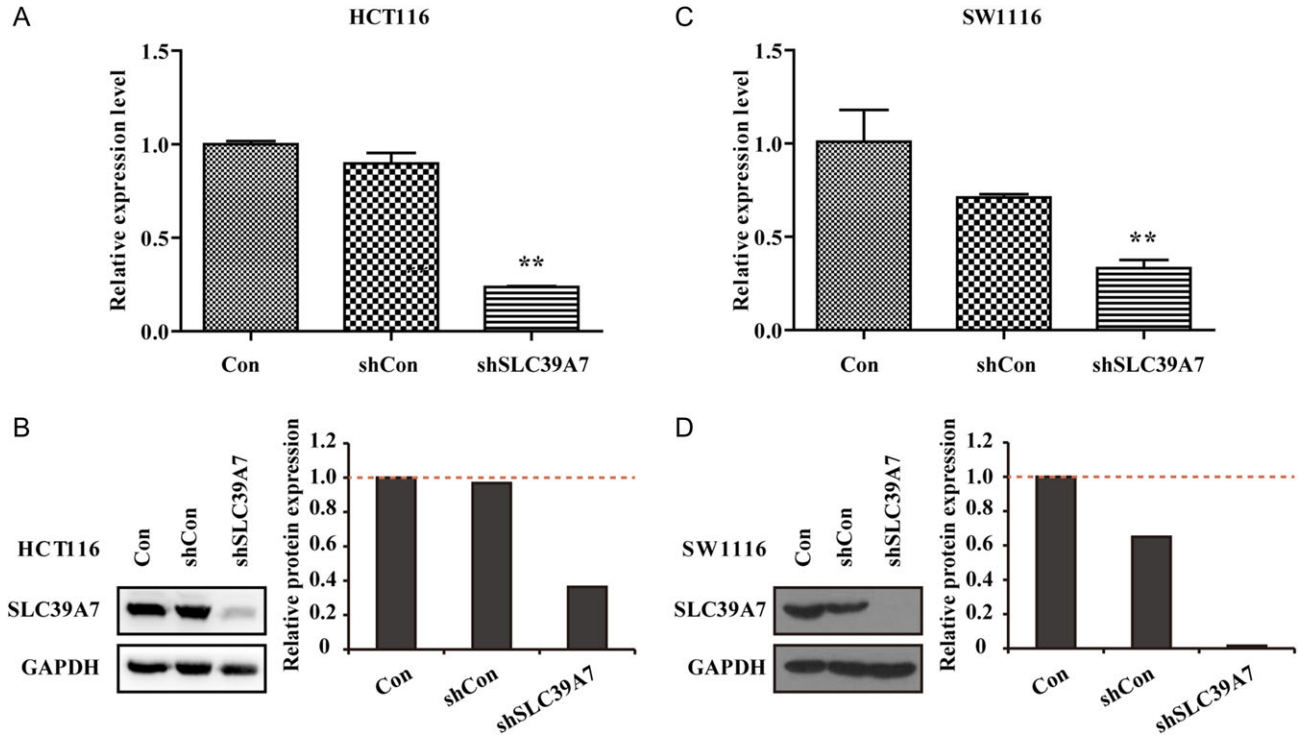

Figure 2. Downregulation of SLC39A7 mRNA and protein expression in colorectal cancer cells by lentivirus-delivered shRNA (A,C) RT-qPCR analysis of SLC39A7 mRNA in HCT116 and SW1116 cells transfected with shSLC39A7 or shCon control; *β-actin* was used as the control. (B,D) Western blot analysis of SLC39A7 protein in HCT116 and SW1116 cells transfected with shSLC39A7 or shCon control; GAPDH protein was used as an internal control. Data are presented as the mean ± SD ($n = 3$). $^{**}P < 0.01$.

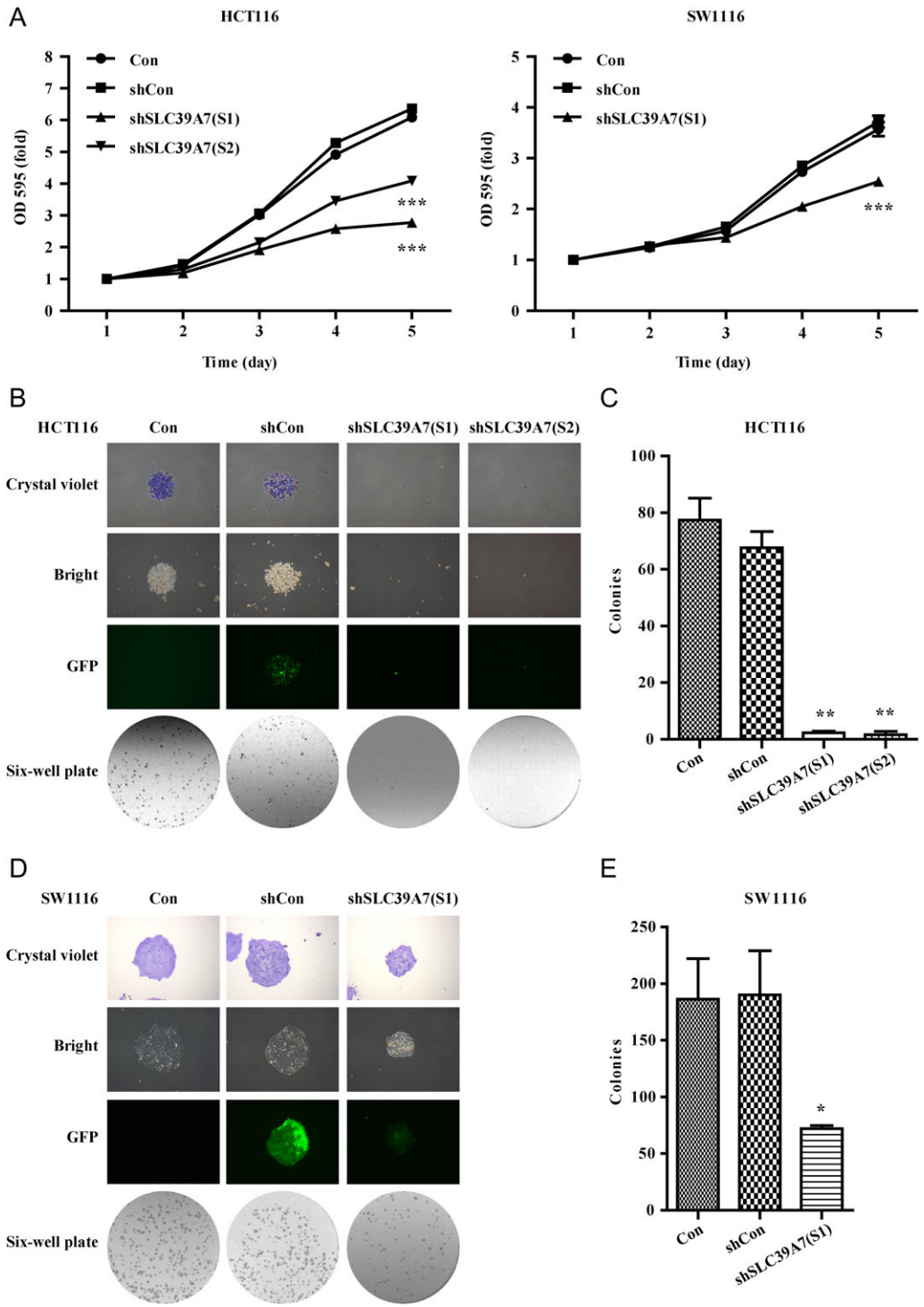

Figure 3. Knockdown of SLC39A7 attenuated proliferation and colony formation of colorectal cancer HCT116 and SW1116 cells (A) Growth inhibition curves for the shSLC39A7-transfected HCT116 and SW1116 cells. (B,D) Representative images of crystal violet stained colonies were captured. ShSLC39A7 transfection resulted in formation of smaller and fewer colonies; scale bar = 250 μm. (C,E) The number of colonies form by cells transfected with shSLC39A7 was much fewer than those transfected with shCon. Data are presented as the mean ± SD ($n = 3$). *$P < 0.05$, **$P < 0.01$, and ***$P < 0.001$.

the number of colonies in SW1116 cells transfected with shSLC39A compared with shCon control (**Fig. 3E**). These results indicated that knockdown of SLC39A7 attenuated colony-forming activity of HCT116 and SW1116 cells.

Knockdown of SLC39A7-induced cell cycle arrest

To explore the possible mechanism mediating the inhibitory effect of SLC39A7 knockdown on colorectal cancer cells growth, cell cycle distribution was analyzed by flow cytometry assay (**Fig. 4A**). As

shown in **Fig. 4B**, transfection with shSLC39A7 significantly decreased the percentage of HCT116 cells in S phase (19.26% vs. 30.08%, $P < 0.001$) and increased the percentage of HCT116 cells in G2/M phase (19.87% vs. 12.65%, $P < 0.01$) compared with shCon-transfected cells. Meanwhile, the percentage of SW1116 cells in the S phase was decreased from 34.47% in the shCon-transfected group to 27.31% in the shSLC39A7-transfected group, and the percentage of SW1116 cells in the G2/M phase was increased from 3.49% to 10.05% (**Fig. 4C**). These results showed that knockdown of SLC39A7 induced colorectal cancer cells apoptosis and arrested cells at the G2/M phase.

Knockdown of SLC39A7 boosted cell apoptosis

To further investigate the effects of SLA39A7 downregulation on the colorectal cancer cell apoptosis, Annexin V-APC/7AAD double staining was performed (**Fig. 5A**). Compared with the control, the percentage of early and late apoptotic cells in shSLC39A7-transfected HCT116 cells was significantly increased from 1.01% to 12.20% and from 4.05% to 19.53%, respectively, as evidenced by Annexin V+/7AAD– and Annexin V+/7AAD+ staining (**Fig. 5B**). A similar phenomenon was observed in the SW1116 cells transfected with shSLC39A7 (**Fig. 5C**; $P < 0.001$). These results suggested that knockdown of SLC39A7 induced early and late apoptosis progression in colorectal cancer cells.

Knockdown of SLC39A7 altered the expressions of apoptosis-related proteins

To reveal the molecular basis for cell apoptosis caused by SLC39A7 knockdown, the expression levels of several apoptosis-related proteins were determined by western blot analysis. Our results showed that shSLC39A7 treatment obviously promoted the cleavage of PARP and enhanced the expression levels of Bad, Caspase-9 and cleaved-Caspase-3, but suppressed Bcl-2 expression (**Fig. 6**).

Discussion

Colorectal cancer is one of the most common malignancy worldwide, and the poor survival rate is mainly due to late-stage diagnosis of this aggressive disease and limited effectiveness of currently available treatment strategies [14]. Hence, a better understanding of the

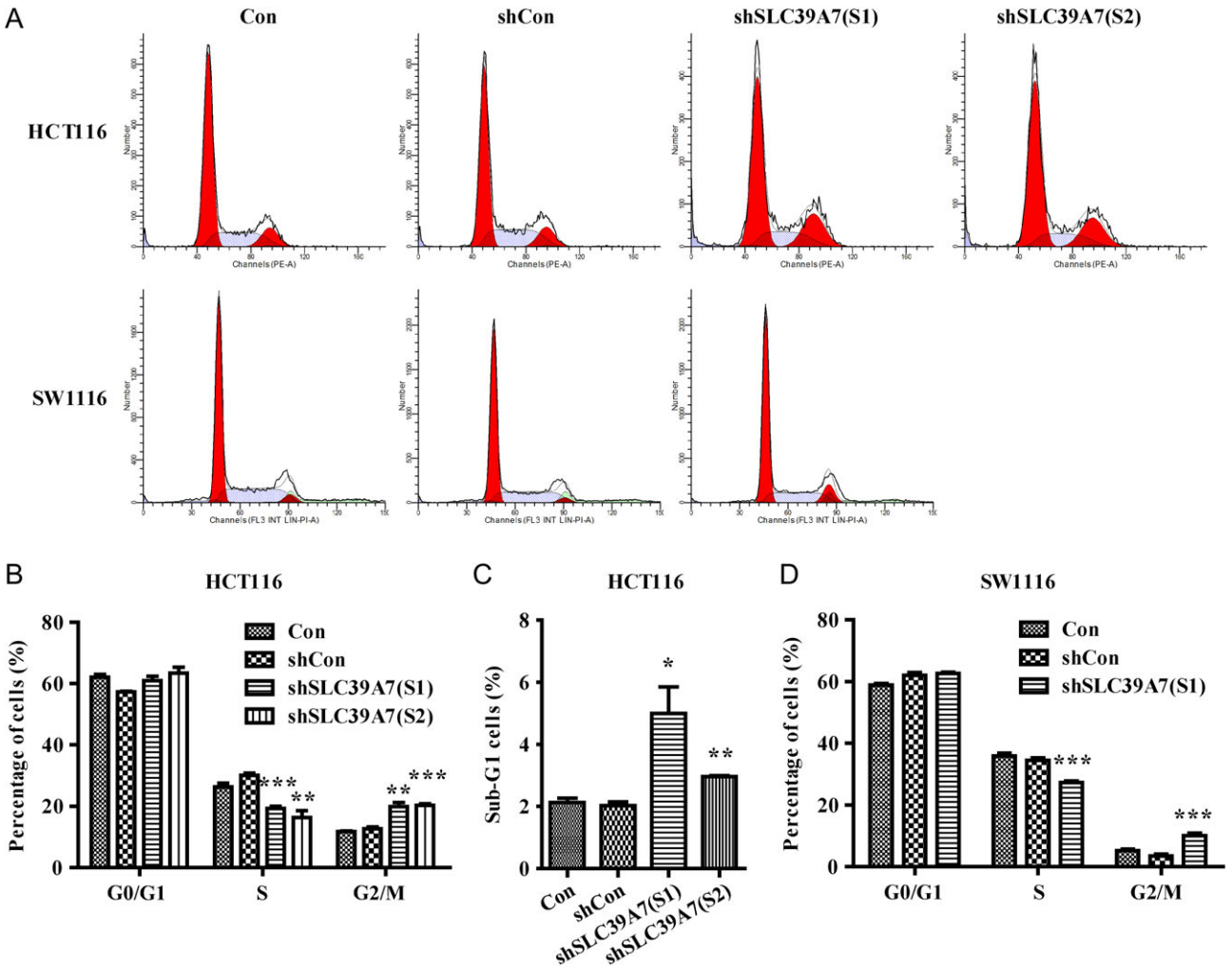

Figure 4. Knockdown of SLC39A7 induced G2/M cell cycle arrest in colorectal cancer HCT116 and SW1116 cells (A) Representative histograms showing the cell cycle distribution of normal cells, shCon-transfected and ShSLC39A7-transfected colorectal cancer HCT116 and SW1116 cells. (B–D) ShSLC39A7 transfection decreased the percentage of cells in S phase and increased cells in G2/M phase. Data are presented as the mean ± SD ($n = 3$). $^{*}P < 0.05$, $^{**}P < 0.01$, and $^{***}P < 0.001$.

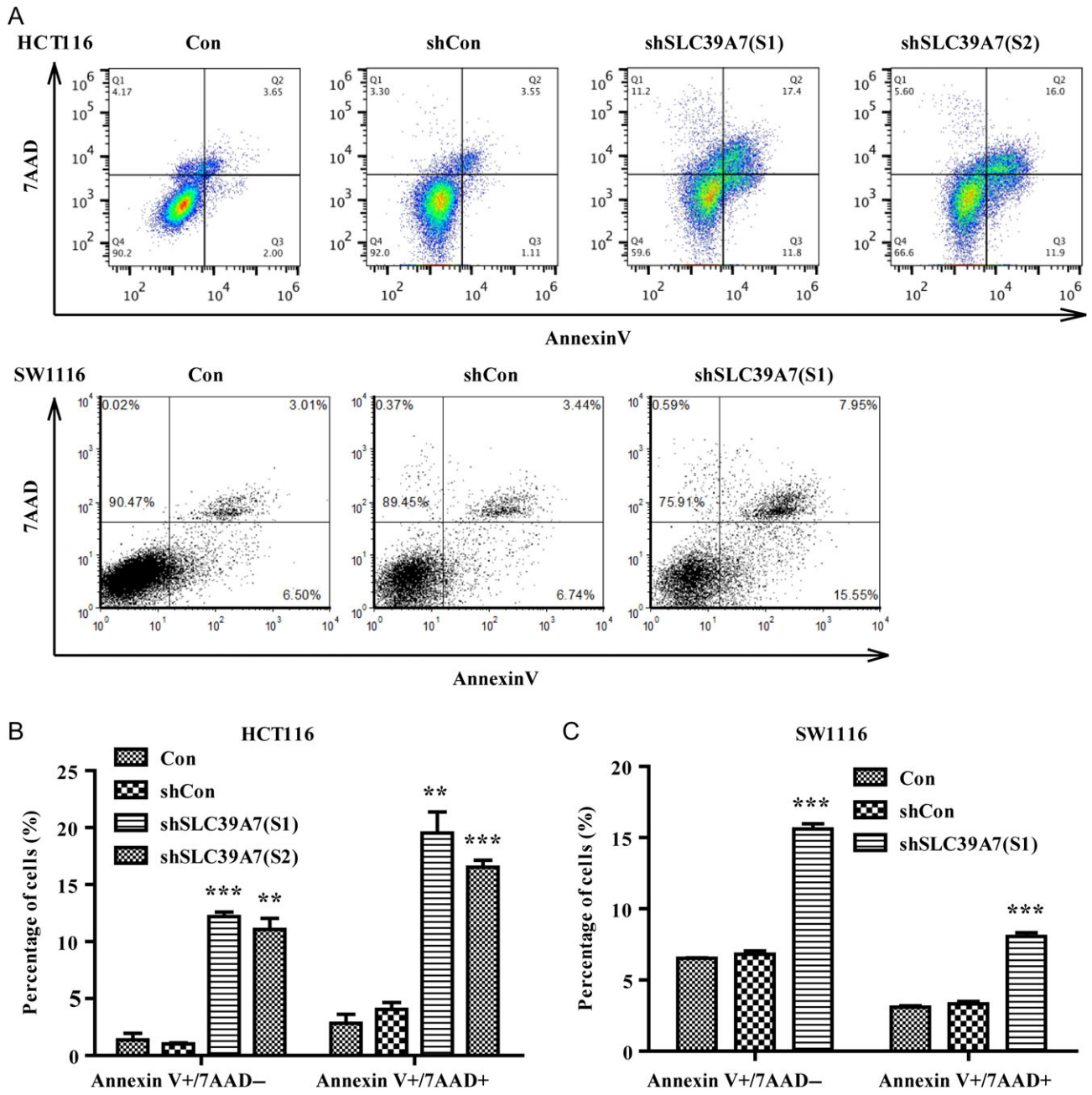

Figure 5. Knockdown of SLC39A7 induced early and late apoptosis in colorectal cancer HCT116 and SW1116 cells (A) Representative histograms depicting apoptosis in of normal cells, shCon-transfected and ShSLC39A7-transfected colorectal cancer HCT116 and SW1116 cells. (B,C) Statistical analysis of the percentage of HCT116 and SW1116 cells in early and late stages of apoptosis. Data are presented as the mean ± SD ($n = 3$). $^{**}P < 0.01$, and $^{***}P < 0.001$.

molecular mechanisms of colorectal cancer will facilitate the development of new treatment modalities. In the present study, we found that the zinc transporter, SLC39A7 is implicated in human colorectal cancer tumorigenesis and progression. SLC39A7 was found to be highly expressed in colorectal cancer tissues in comparison with normal tissues. SLC39A7 shRNA-expressing lentivirus was used to silence its endogenous expression in two colorectal cancer cell lines, i.e. HCT116 and SW1116. MTT and colony-forming assay demonstrated that SLC39A7 knockdown inhibited cell viability and proliferation, indicating a tumor-promoting function of SLC39A7 in colorectal cancer.

To elucidate the mechanism of the tumor-promoting function of SLC39A7, cell cycle distribution analysis was determined. The results showed that knockdown of SLC39A7 arrested HCT116 and SW1116 cells in the G2/M phase with decreased percentage of cells in the S phase. The cell cycle is made up of a series of specific events that drive mitotic cell division and DNA replication [15]. Cell cycle distribution at different stages is strictly regulated by cyclin/cyclin-dependent kinase (CDK) complexes [16]. For example, cyclin E, cyclin D1/CDK4 and -6 are required for the G1 to S phase transition [17]. The CDK1/cyclin A and -B complex are essential for cells to enter M phase and the CDK2/cyclin A controls the progression through

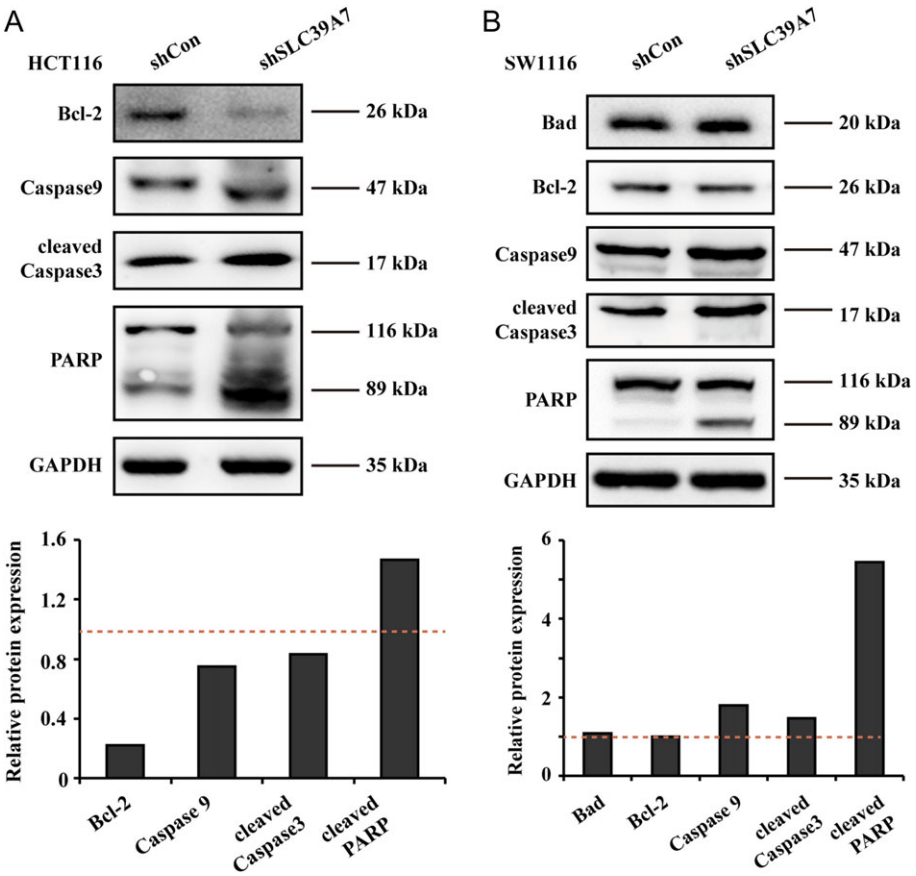

Figure 6. Knockdown of SLC39A7 altered expression of apoptosis-related proteins in colorectal cancer cells Apoptosis-related proteins were detected by western blot analysis using their corresponding antibodies. (A) Expression of apoptosis-related proteins in the HCT116 cells of shCon, shSLC39A7 groups. (B) Expression of apoptosis markers in the SW1116 cells of shCon and shSLC39A7 groups. GAPDH protein was used as an internal control.

the S phase [18]. We supposed that knockdown of SLC39A7 may induce cell cycle arrest at G2/M phase possibly through regulation of CDK/cyclin complexes, especially CDK1-cyclin A or cyclin B or both. We also observed that HCT116 cells with SLC39A7 knockdown exhibited a large sub G1 peak, a sign of apoptosis (**Supplementary Fig. S2**). To further evaluate the effect of SLC39A7 on apoptosis, Annexin V-APC/7AAD double staining was performed, and results showed that downregulation of SLC39A7 resulted in early and late apoptosis in both HCT116 and SW1116 cells. The regulatory mechanism for the apoptotic effect of SLC39A7 in colorectal cancer cells was further evaluated. It has been shown that there are numerous stimuli functions to trigger apoptotic cell death, and two major apoptotic pathways are present in higher eukaryotes, i.e. the death receptor pathway and the mitochondrial pathway [19]. In mitochondrial apoptosis, downregulation of Bcl-2 (anti-apoptotic molecule) often occurs, thereby triggering the pro-apoptotic BAX and BAK oligomerization and forming pores in the mitochondrial membrane to release cytochrome *c* into the cytoplasm [20]. Cytochrome c release from the mitochondria leads to the formation of apoptosome, followed by activation of caspase 9 and cleaved-caspase 3 [21]. Cleaved-caspase 3 is considered as a key executioner of apoptosis, which on activation results in cleavage of PARP and provokes the systematic dismantling of cell into apoptotic bodies [22]. In the present study, the increase in Bad, caspase 9, and cleaved-caspase 3 and decrease in Bcl-2 as well as cleavage of PARP were observed in both HCT116 and SW1116 cells. Our data suggest that apoptosis in colorectal cancer cells induced by SLC39A7 knockdown is mediated through the activation of caspases cascade and the mitochondrial pathway.

SLC39A7 functions as zinc transporter that releases zinc from the endoplasmic reticulum and appears to be essential for the activation of tyrosine kinase [23]. Increased levels of zinc and ZIP7 were found in the tamoxifen-resistant breast cancer MCF-7 cells. These cells display an aggressive and invasive phenotype through zinc-induced activation of receptor tyrosine kinases of EGFR, IGF-1R, and nonreceptor tyrosine kinases Src [8]. Conversely, the removal of SLC39A7 blocks the zinc-induced activation of EGFR, IGF-1R, and Src, thereby destroying the activation of AKT, HER-2, HER-3, and HER-4 [8]. The EGFR and IGF-1R are known to transmit signals to prominent downstream pathways, such as RAS/RAF/MAPK and PI3K/AKT/mTOR signaling pathways which are involved in cell proliferation and survival [24]. A previous report revealed that there is a functional synergism between proto-oncogene Src and HER-2 for the acceleration of breast cancer progression [25]. Src is also an activator of JAK-STAT signaling which promotes cell proliferation, differentiation, migration, and survival [26]. In this study, after knockdown of SLC39A7 in colorectal cancer cells, the zinc-stimulated activation of receptor and nonreceptor tyrosine kinases, as well as some other molecules associated with aggressive and invasive cell behavior might be prevented. Furthermore, we supposed that the signaling pathways including RAS/RAF/MAPK, PI3K/AKT/mTOR, and JAK/STAT might be blocked, which contributed to the

induction of mitochondria-dependent apoptotic pathway and G2/M cell cycle arrest.

In conclusion, our investigation demonstrated that knockdown of SLC39A7 suppressed the growth of colorectal cancer cells though G2/M cell cycle arrest and apoptosis. Our findings suggested that SLC39A7 might function as a potential oncogene that plays an important role in colorectal cancer occurrence and development. Expression and functional identification of SLC39A7 in colorectal cancer will help us to understand the molecular mechanism of oncogenesis in colorectal cancer. This may facilitate the exploration of novel therapeutic agents for improving clinical outcome in patients.

Supplementary Data

Supplementary data are available at *Acta Biochimica et Biophysica Sinica* online.

Funding

This work was supported by the grants from the National Natural Science Foundation of China (No. 81372311) and Shanghai Municipal Commission of Health and Family Planning Research Projects (No. 20134024).

References

1. Siegel RL, Miller KD, Jemal A. Cancer Statistics, 2017. *CA Cancer J Clin* 2017, 67: 7–30.
2. Siegel RL, Miller KD, Fedewa SA, Ahnen DJ, Meester RGS, Barzi A, Jemal A. Colorectal cancer statistics, 2017. *CA Cancer J Clin* 2017, 67: 177–193.
3. Brenner H, Kloor M, Pox CP. Colorectal cancer. *Lancet* 2014, 383: 1490–1502.
4. Franklin RB, Costello LC. The important role of the apoptotic effects of zinc in the development of cancers. *J Cell Biochem* 2009, 106: 750–757.
5. Beyersmann D, Haase H. Functions of zinc in signaling, proliferation and differentiation of mammalian cells. *Biometals* 2001, 14: 331–341.
6. Yan G, Zhang Y, Yu J, Yu Y, Zhang F, Zhang Z, Wu A, *et al*. Slc39a7/zip7 plays a critical role in development and zinc homeostasis in zebrafish. *PLoS ONE* 2012, 7: e42939.
7. Huang L, Kirschke CP, Zhang Y, Yu YY. The ZIP7 gene (Slc39a7) encodes a zinc transporter involved in zinc homeostasis of the Golgi apparatus. *J Biol Chem* 2005, 280: 15456–15463.
8. Taylor KM, Vichova P, Jordan N, Hiscox S, Hendley R, Nicholson RI. ZIP7-mediated intracellular zinc transport contributes to aberrant growth factor signaling in antihormone-resistant breast cancer Cells. *Endocrinology* 2008, 149: 4912–4920.
9. Ohashi W, Kimura S, Iwanaga T, Furusawa Y, Irie T, Izumi H, Watanabe T, *et al*. Zinc transporter SLC39A7/ZIP7 promotes intestinal epithelial self-renewal by resolving ER stress. *PLoS Genet* 2016, 12: e1006349.
10. Taylor KM, Hiscox S, Nicholson RI, Hogstrand C, Kille P. Protein kinase CK2 triggers cytosolic zinc signaling pathways by phosphorylation of zinc channel ZIP7. *Sci Signal* 2012, 5: ra11.
11. Kaiser S, Park YK, Franklin JL, Halberg RB, Yu M, Jessen WJ, Freudenberg J, *et al*. Transcriptional recapitulation and subversion of embryonic colon development by mouse colon tumor models and human colon cancer. *Genome Biol* 2007, 8: R131.
12. Ki DH, Jeung HC, Park CH, Kang SH, Lee GY, Lee WS, Kim NK, *et al*. Whole genome analysis for liver metastasis gene signatures in colorectal cancer. *Int J Cancer* 2007, 121: 2005–2012.
13. Rhodes DR, Kalyana-Sundaram S, Mahavisno V, Varambally R, Yu J, Briggs BB, Barrette TR, *et al*. Oncomine 3.0: genes, pathways, and networks in a collection of 18,000 cancer gene expression profiles. *Neoplasia* 2007, 9: 166–180.
14. Alberts SR, Horvath WL, Sternfeld WC, Goldberg RM, Mahoney MR, Dakhil SR, Levitt R, *et al*. Oxaliplatin, fluorouracil, and leucovorin for patients with unresectable liver-only metastases from colorectal cancer: a North Central Cancer Treatment Group phase II study. *J Clin Oncol* 2005, 23: 9243–9249.
15. Caldon CE, Daly RJ, Sutherland RL, Musgrove EA. Cell cycle control in breast cancer cells. *J Cell Biochem* 2006, 97: 261–274.
16. Vlach J, Hennecke S, Amati B. Phosphorylation-dependent degradation of the cyclin-dependent kinase inhibitor p27. *EMBO J* 1997, 16: 5334–5344.
17. Megha T, Lazzi S, Ferrari F, Vatti R, Howard CM, Cevenini G, Leoncini L, *et al*. Expression of the G2-M checkpoint regulators cyclin B1 and P34CDC2 in breast cancer: a correlation with cellular kinetics. *Anticancer Res* 1999, 19: 163–169.
18. Huang S, Lin R, Yu Y, Lu Y, Connolly PJ, Chiu G, Li S, *et al*. Synthesis of 3-(1H-benzimidazol-2-yl)-5-isoquinolin-4-ylpyrazolo[1,2-b]pyridine, a potent cyclin dependent kinase 1 (CDK1) inhibitor. *Bioorg Med Chem Lett* 2007, 17: 1243–1245.
19. Gupta S. Molecular steps of death receptor and mitochondrial pathways of apoptosis. *Life Sci* 2001, 69: 2957–2964.
20. Gallerne C, Prola A, Lemaire C. Hsp90 inhibition by PU-H71 induces apoptosis through endoplasmic reticulum stress and mitochondrial pathway in cancer cells and overcomes the resistance conferred by Bcl-2. *Biochim Biophys Acta* 2013, 1833: 1356–1366.
21. Chen J, Wang L, Wu C, Hu Q, Gu C, Yan F, Li J, *et al*. Melatonin-enhanced autophagy protects against neural apoptosis via a mitochondrial pathway in early brain injury following a subarachnoid hemorrhage. *J Pineal Res* 2014, 56: 12–19.
22. Liu J, Wu Y, Wang B, Yuan X, Fang B. High levels of glucose induced the caspase-3/PARP signaling pathway, leading to apoptosis in human periodontal ligament fibroblasts. *Cell Biochem Biophys* 2013, 66: 229–237.
23. Hogstrand C, Kille P, Nicholson RI, Taylor KM. Zinc transporters and cancer: a potential role for ZIP7 as a hub for tyrosine kinase activation. *Trends Mol Med* 2009, 15: 101–111.
24. Gong Y, Yao E, Shen R, Goel A, Arcila M, Teruya-Feldstein J, Zakowski MF, *et al*. High expression levels of total IGF-1R and sensitivity of NSCLC cells in vitro to an anti-IGF-1R antibody (R1507). *PLoS ONE* 2009, 4: e7273.
25. Biscardi JS, Ishizawar RC, Silva CM, Parsons SJ. Tyrosine kinase signalling in breast cancer: epidermal growth factor receptor and c-Src interactions in breast cancer. *Breast cancer Res* 2000, 2: 203–210.
26. Rawlings JS, Rosler KM, Harrison DA. The JAK/STAT signaling pathway. *J Cell Sci* 2004, 117: 1281–1283.